Energy Level Tuning of Poly(phenylene-*alt*-dithienobenzothiadiazole)s for Low Photon Energy Loss Solar Cells

Ruurd Heuvel, Jacobus J. van Franeker, René A. J. Janssen*

Six poly(phenylene-*alt*-dithienobenzothiadiazole)-based polymers have been synthesized for application in polymer–fullerene solar cells. Hydrogen, fluorine, or nitrile substitution on benzothiadiazole and alkoxy or ester substitution on the phenylene moiety are investigated to reduce the energy loss per converted photon. Power conversion efficiencies (PCEs) up to 6.6% have been obtained. The best performance is found for the polymer–fullerene combination with distinct phase separation and crystalline domains. This improves the maximum external quantum efficiency for charge formation and collection to 66%. The resulting higher photocurrent compensates for the relatively large energy loss per photon (E_{loss} = 0.97 eV) in achieving a high PCE. By contrast, the polymer that provides a reduced energy loss (E_{loss} = 0.49 eV) gives a lower photocurrent and a reduced PCE of 1.8% because the external quantum efficiency of 17% is limited by a suboptimal morphology and a reduced driving force for charge transfer.

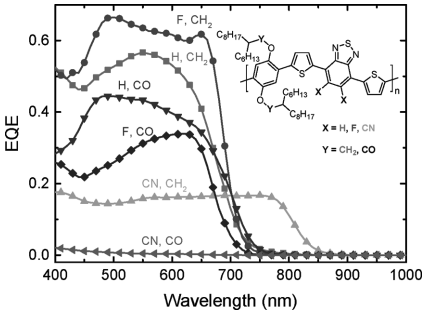

1. Introduction

In the search for new, efficient materials for polymer solar cells medium (1.7–1.4 eV)[1–3] and small (<1.4 eV)[4–10] optical band gap (E_g) materials have attracted considerable attention. For these materials good efficiencies have been obtained, sometimes even without the need for special processing conditions such as halogenated solvents[11] or cosolvents.[12] For the best performing materials, that feature optical band gaps around 1.55 eV, the power conversion efficiency (PCE) already exceeds 10%. At 1.55 eV, the optical band gap is low enough to absorb a considerable part of the solar spectrum, resulting in a high short-circuit current (J_{sc}) and at the same time high enough to maintain an open-circuit voltage (V_{oc}) around 0.8 V. Smaller optical band gap materials are mainly used as the bottom layer in multijunction devices,[10,13–15] where the near infrared part of the solar spectrum is converted, albeit at a lower voltage. In order to make optimal use of the solar spectrum in tandem and triple-junction solar cells, more efficient wide band gap materials are required.

Conjugated polymers based on benzothiadiazole (BT) have been shown to provide efficient solar cells for both the medium and wide band gap range. You and co-workers[16,17] showed that, by substituting 2,1,3-benzothiadiazole with fluorine in the 5 and 6 positions, both the highest occupied molecular orbital (HOMO) and lowest unoccupied

R. Heuvel, Dr. J. J. van Franeker, Prof. R. A. J. Janssen
Molecular Materials and Nanosystems
Institute for Complex Molecular Systems
Eindhoven University of Technology
P.O. Box 513, 5600 MB, Eindhoven, The Netherlands
E-mail: r.a.j.janssen@tue.nl
Dr. J. J. van Franeker
Dutch Polymer Institute
P.O. Box 902, 5600 AX, Eindhoven, The Netherlands
Prof. R. A. J. Janssen
Dutch Institute for Fundamental Energy Research
De Zaale 20, 5612 AJ, Eindhoven, The Netherlands

DOI: 10.1002/macp.201600502

molecular orbital (LUMO) could be lowered effectively. This resulted in a higher V_{oc} while maintaining the band gap. Woo and co-workers[18] used this knowledge to develop a highly efficient wide band gap material, with a maximum performance of 9.4% PCE at a band gap of 1.76 eV. To further increase the efficiency of these polymers, the photon energy loss (E_{loss}) upon charge separation should be minimized while ensuring a sufficiently large driving force for the separation of charges. The role of the photon energy loss, defined as $E_{loss} = E_g - qV_{oc}$ (with q the elementary charge), in polymer solar cells has been studied before.[19–21] Generally a rapid drop in external quantum efficiency (EQE) is observed when E_{loss} drops below 0.6 eV, resulting in very low PCEs.

This work focuses on investigating the possibilities of decreasing the photon energy loss of the poly(phenylene-*alt*-dithienobenzothiadiazole)-based polymers introduced by Woo and co-workers[18] and finding the limit in which charge separation is still efficient. For this purpose, six different poly(phenylene-*alt*-dithienobenzothiadiazole)s are compared by introducing electron withdrawing or donating substituents on benzothiadiazole and phenylene. For benzothiadiazole, we investigate the effect of hydrogen (BT), fluorine (FBT), and nitrile (NBT) substituents on the 5 and 6 positions and show that the increasingly more electron withdrawing nature of the substituent is able to tune the energy levels of the polymer. We note that while this work was in progress, Woo and co-workers published the effect of introducing two nitrile substituents on benzothiadiazole.[22] Replacing the alkoxy side chains on the phenylene for more electron deficient ester analogues results in a similar effect on the electron rich donor block.

2. Experimental Section

2.1. Materials and Methods

Tris(dibenzylideneacetone)dipalladium (Pd_2dba_3) (Strem Chemicals Inc.), 4,7-dibromobenzo[c][1,2,5]thiadiazole, and 4,7-dibromo-5,6-difluorobenzo[c][1,2,5]thiadiazole (SunaTech Inc.) were used as received. Triphenylphosphine (PPh_3) was recrystallized from absolute ethanol. All solid monomers were freshly recrystallized prior to use, liquid monomers were subjected to column chromatography and used within 2 d. 4,7-Di(thiophen-2-yl)-benzo[c][1,2,5]thiadiazole(**1**),5,6-difluoro-4,7-di(thiophen-2-yl)benzo[c]-[1,2,5]thiadiazole (**2**), 4,7-di(thiophen-2-yl)benzo[c][1,2,5]thiadiazole-5,6-dicarbonitrile (**3**), 4,7-bis(5-(trimethylstannyl)thiophen-2-yl)benzo[c][1,2,5]thiadiazole (**M1**), and 5,6-difluoro-4,7-bis(5-(trimethylstannyl)thiophen-2-yl)benzo[c][1,2,5]thiadiazole (**M2**) were synthesized according to literature procedures.[18, 23–25]

^{1}H and ^{13}C NMR spectra were recorded at respectively 400 and 100 MHz on a Varian Mercury spectrometer at 25 °C. Molecular weights of small molecules were determined using matrix assisted laser desorption ionization time of flight (MALDI-TOF) mass spectroscopy (MS) (Bruker Autoflex Speed spectrometer) or gas chromatography/MS (GC-MS) (Shimadzu GC-2010 chromatograph, equipped with a Zebron ZB-5MS column and a GCMS-QP2010 plus mass spectrometer). Molecular weights of polymers were determined by gel permeation chromatography (GPC) on a Polymer Laboratories (PL) GPC 220 using a PL-GEL 10 μm MIXED-B column. The system was operated at 140 °C with *o*-dichlorobenzene (oDCB) as the eluent. Samples, dissolved at 0.1 mg mL^{-1}, were measured against polystyrene standards. UV/visible/NIR spectroscopy was conducted on a PerkinElmer Lambda 1050 spectrophotometer equipped with a photomultiplier tube/InGaAs/PbS three-detector module. Cyclic voltammetry was carried out using an AutoLab PGSTAT 30 in an inert atmosphere. The electrolyte consisted of 0.1 M tetrabutylammonium hexafluorophosphate (TBA^+ PF_6^-) in acetonitrile. The sample was applied as a thin film, spin coated on an indium tin oxide (ITO) coated glass substrate as working electrode. A silver rod was used as counter electrode and a silver chloride coated silver rod (Ag/AgCl) was used as quasi-reference electrode. The measurements were performed at a scan speed of 0.1 V s^{-1} and potentials are quoted versus Fc/Fc^+ as external standard. For conversion to energy levels versus vacuum we used $E_{Fc/Fc+} = -5.0$ eV.

Photovoltaic devices were fabricated with active areas of 0.09 and 0.16 cm^2. Poly(ethylenedioxythiophene):poly(styrenesulfonate) (PEDOT:PSS) (Clevios P, VP Al4083) was spin coated on precleaned, patterned ITO/glass substrates (Naranjo Substrates). The active layer was spin coated at 2000 rpm from either a chloroform(/cosolvent) solution (6 mg mL^{-1} polymer, 9 mg mL^{-1} [6,6]-phenyl-C_{71}-butyric acid methyl ester ($PC_{71}BM$)) or a chlorobenzene(/cosolvent) solution (11 mg mL^{-1} polymer, 16.7 mg mL^{-1} $PC_{71}BM$). The back electrode was evaporated at ≈10^{-7} mbar and consisted of LiF (1 nm) and Al (100 nm) layers. Current density–voltage (*J*–*V*) characteristics were recorded with a Keithley 2400 source meter using a tungsten-halogen lamp as light source. The light was filtered by a Schott GG385 UV filter and a Hoya LB120 daylight filter to provide 100 mW cm^{-2} AM1.5G light. Short-circuit currents and PCEs were calculated by integrating the solar spectrum and the spectral response of the cells. EQEs were determined using modulated monochromatic light from a 50 W tungsten-halogen lamp (Philips Focusline) passing through a monochromator (Oriel, Cornerstone 130) and a mechanical chopper. The response was recorded as the voltage produced by a preamplifier (Stanford Research Systems SR570) with a lock-in amplifier (SR830). All measurements were done against an Si-reference cell with known spectral response. Transmission electron microscopy (TEM) was performed on a Tecnai G2 Sphera transmission electron microscope (FEI) operating at 200 kV. Layer thicknesses were determined using a Vecoo Dektak 150 profilometer, subtracting the thickness of any underlying layers.

2.2. Synthesis

2.2.1. 7-(Bromomethyl)pentadecane (4)

2-Hexyldecan-1-ol (30.0 g, 123 mmol) and PPh_3 (36.0 g, 137 mmol) were dissolved in dichloromethane (150 mL) and cooled to 0 °C. *N*-Bromosuccinimide (22.3 g, 125 mmol) was added in portions. The reaction mixture was allowed to warm to room temperature

and stirred for 70 min in the dark. Heptane was added and the organic phase washed with water. Dichloromethane was evaporated and the mixture filtered through a silica plug. All solvents were evaporated, heptane added, and the mixture again filtered through a silica plug. All solvents were evaporated to obtain the product as a transparent, colorless oil in a yield of 34.6 g (113 mmol or 91.6%). ^{1}H-NMR (400 MHz, $CDCl_3$, δ) 3.45 (d, J = 4.8 Hz, 2H); 1.60 (m, 1H); 1.28 (m, 24H); 0.89 (m, 6H). ^{13}C-NMR (100 MHz, $CDCl_3$, δ) 39.66; 39.52; 32.59; 31.91; 31.83; 29.81; 29.57; 29.48; 29.32; 26.58; 22.67; 14.10. GC-MS: $[M\text{-}Br]^+$ calc: 225.26, found: 225.30.

2.2.2. 4,7-Bis(5-(trimethylstannyl)thiophen-2-yl)benzo[c]-[1,2,5]thiadiazole-5,6-dicarbonitrile (**M3**)

4,7-Di(thiophen-2-yl)benzo[c][1,2,5]thiadiazole-5,6-dicarbonitrile (**3**) (0.296 g, 0.845 mmol) was dissolved in tetrahydrofuran (45 mL) in a dry three-necked flask under argon atmosphere. The solution was cooled to −78 °C and a 2 M lithium diisopropylamide solution in tetrahydrofuran (3.8 mL, 7.6 mmol) was added dropwise. The mixture was stirred for 1 h at −78 °C, after which a 1 M trimethyltin chloride solution in tetrahydrofuran (8.0 mL, 8.0 mmol) was added dropwise. The reaction mixture was stirred for another hour at −78 °C, after which water was added to quench the reaction. The mixture was then allowed to warm to room temperature. The product was extracted with diethyl ether and washed with water and brine. The organic phase was dried over anhydrous magnesium sulfate and concentrated in vacuum to obtain the crude product. Further purification was carried out by multiple recrystallizations in methanol and ethanol to obtain the product as small red crystals at a yield of 0.338 g (0.500 mmol or 59%). ^{1}H-NMR (400 MHz, $CDCl_3$, δ) 8.24 (d, J = 3.6 Hz, 2H); 7.37 (d, J = 3.5 Hz, 2H); 0.47 (t, J = 28.4 Hz, 18H). ^{13}C-NMR (100 MHz, $CDCl_3$, δ) 153.48; 147.46; 138.58; 135.69; 133.13; 133.02; 116.44; 110.24; −7.99. MALDI-TOF-MS: $[M\text{-}CH_3]^+$ calc: 660.88, found: 660.89.

2.2.3. 1,4-Dibromo-2,5-bis((2-hexyldecyl)oxy)benzene (**M4**)

Potassium carbonate (1.10 g, 7.96 mmol) was suspended in a solution of 7-(bromomethyl)pentadecane (**4**) (2.48 g, 8.11 mmol) and 2,5-dibromobenzene-1,4-diol (1.01 g, 3.77 mmol) in dichloromethane (15 mL) in a dry Schlenk flask under argon atmosphere. The suspension was degassed by bubbling with argon for 15 min. The tube was sealed and 5 pumps per purge cycles were performed to remove any remaining oxygen. The mixture was then heated to 80 °C overnight. After cooling to room temperature, a 1 M solution of ammonium chloride was added and the product extracted with heptane. The organic layer was washed with 1 M ammonium chloride solution and water, dried over magnesium sulfate, and concentrated in vacuum. The crude product was subjected to column chromatography (silica, heptane) affording the pure product as a transparent colorless oil, with a yield of 1.35 g (1.88 mmol or 50%). ^{1}H-NMR (400 MHz, $CDCl_3$, δ) 7.07 (s, 2H); 3.82 (d, J = 5.6 Hz, 4H); 1.80 (m, 2H); 1.29 (m, 48H); 0.89 (m, 12H). ^{13}C-NMR (100 MHz, $CDCl_3$, δ) 150.17; 118.19; 111.06; 72.95; 37.96; 31.92; 31.85; 31.32; 31.31; 30.00; 29.67; 29.58; 29.34; 26.82; 26.79; 22.69; 14.13. MALDI-TOF-MS: $[M]^+$ calc: 714.36, found: 714.37.

2.2.4. 2,5-Dibromo-1,4-phenylene bis(2-hexyldecanoate) (**M5**)

2,5-Dibromobenzene-1,4-diol (0.60 g, 2.2 mmol) was dissolved in tetrahydrofuran (10 mL) and cooled to 0 °C. Pyridine (0.4 mL) and 2-hexyldecanoyl chloride (1.5 g, 5.38 mmol) were added dropwise. The mixture was stirred for 10 min at 0 °C and then allowed to warm to room temperature. Tetrahydrofuran (10 mL) and acetone (20 mL) were added and the mixture stirred for another 4 h at room temperature. All volatiles were evaporated in vacuum and the remaining mixture resuspended in diethyl ether. The solids were washed away with water, after which the combined water phases were once more extracted with diethyl ether. The combined organic phases were washed with a saturated ammonium chloride solution and dried over anhydrous magnesium sulfate. The crude product was then further purified by column chromatography (silica, heptane/dichloromethane 2:1) to obtain the pure product as a transparent, colorless oil with a yield of 0.63 g (0.84 mmol or 38%) . ^{1}H-NMR (400 MHz, $CDCl_3$, δ) 7.35 (s, 2H); 2.62 (m, 2H); 1.79 (m, 4H); 1.59 (m, 4H); 1.30 (m, 40H); 0.89 (m, 12H). ^{13}C-NMR (100 MHz, $CDCl_3$, δ) 173.51; 146.22; 127.76; 114.99; 45.66; 32.21; 31.87; 31.69; 29.55; 29.44; 29.27; 29.22; 27.47; 27.44; 22.68; 22.62; 14.12; 14.08. MALDI-TOF-MS: $[M+Na]^+$ calc: 765.31, found: 765.31.

2.2.5. Polymerization Reactions

PPDTBT: To a dry Schlenk vial equipped with screw cap was added, 1,4-dibromo-2,5-bis((2-hexyldecyl)oxy)benzene (**M4**) (115.4 mg, 0.161 mmol), 4,7-bis(5-(trimethylstannyl)thiophen-2-yl)benzo[c][1,2,5]thiadiazole (**M1**) (101.0 mg, 0.161 mmol), PPh_3 (5.130 mg, 19.56 µmol), Pd_2dba_3 (4.236 mg, 4.626 µmol), anhydrous toluene (3.2 mL), and anhydrous dimethylformamide (DMF) (0.2 mL). The solution was degassed with argon for 15 min and the flask sealed. Five pump purge cycles with argon were performed to remove any remaining oxygen, after which the mixture was heated to 115 °C overnight. The polymer was end capped with tripropyl(thiophen-2-yl)stannane (0.1 mL) and 2-bromothiophene (0.2 mL) heating to 115 °C for 20 min after each addition. The reaction mixture was diluted with chloroform and precipitated in a 1 M solution of HCl in methanol. The resulting solids were further purified using Soxhlet extraction with acetone, hexane, and chloroform. The chloroform fraction was concentrated and precipitated in methanol to obtain PPDTBT as a dark solid (127 mg, yield 89%).

PPDTFBT: **M4** (89.3 mg, 0.125 mmol), **M2** (81.8 mg, 0.124 mmol), PPh_3 (4.02 mg, 15.32 µmol), Pd_2dba_3 (3.28 mg, 3.58 µmol), anhydrous toluene (2.2 mL), and anhydrous DMF (0.2 mL). Yield 101 mg, 91%.

PPDTNBT: **M4** (107.2 mg, 0.150 mmol), **M3** (101.1 mg, 0.150 mmol), PPh_3 (4.641 mg, 17.69 µmol), Pd_2dba_3 (4.006 mg, 4.375 µmol), anhydrous toluene (2.2 mL), and anhydrous DMF (0.2 mL). PPDTNBT was obtained by dissolving the remaining solid in the extraction thimble in hot tetrachloroethane, filtering the hot solution, and precipitating in methanol. Yield 64 mg, 46%.

PPEDTBT: **M5** (180.4 mg, 0.242 mmol), **M1** (152.0 mg, 0.243 mmol), PPh_3 (7.684 mg, 29.30 µmol), Pd_2dba_3 (6.542 mg, 7.144 µmol), anhydrous toluene (3.3 mL), and anhydrous DMF (0.3 mL). Yield 150 mg, 68%.

PPEDTFBT: **M5** (114.8 mg, 0.154 mmol), **M2**, PPh_3 (4.85 mg, 18.5 μmol), Pd_2dba_3 (4.11 mg, 4.49 μmol), anhydrous toluene (2.2 mL), and anhydrous DMF (0.2 mL). **PPEDTFBT** was obtained by dissolving the remaining solid in the extraction thimble in hot tetrachloroethane, filtering the hot solution, and precipitating in methanol. Yield: 104 mg, 71%.

PPEDTNBT: **M5** (110.6 mg, 0.149 mmol), **M3** (100.1 mg, 148 mmol), PPh_3 (4.666 mg, 17.79 μmol), Pd_2dba_3 (4.066 mg, 4.440 μmol), anhydrous toluene (2.2 mL), and anhydrous DMF (0.2 mL). PPEDTNBT was obtained by concentrating and precipitating the dichloromethane fraction (following the hexane fraction). Yield: 137 mg, 95%.

3. Results and Discussion

3.1. Synthesis and Characterization

The synthesis of the monomers and polymers are outlined in Schemes 1 and 2. For preparing monomers **M1**, **M2**, and **M4**, we adapted routes published by Woo and co-workers[18] For the conversion of 5,6-difluoro-4,7-di-2-thienyl-2,1,3-benzothiadiazole **2** to its dinitrile analogue **3** (Scheme 1), we used the route reported by Heeney and co-workers[26,27] Subsequent conversion of **3** to the distannyl monomer **M3** was performed analogous to ref.[18] with some minor changes to cope with decreased reactivity and product stability. Synthesis of the 2,5-dibromo-1,4-phenylene diester **M5** was achieved by preparing acid chloride **5** and reacting it with 2,5-dibromohydroquinone.

Six different PPDTBT polymers were synthesized using palladium-catalyzed Stille-type polycondensation reactions (Scheme 2). The polymers were end capped using monofunctionalized 2-bromothiophene and 2-(trimethylstannyl)thiophene.

The resulting PPDTBT polymers were purified by precipitation and Soxhlet extraction using different solvents and analyzed using high temperature (140 °C) GPC in oDCB. All polymers are sufficiently soluble under these conditions showing no sign of aggregation using in-line recorded UV-vis spectra. The number average molecular weights (M_n) of the PPDTBT polymers are within a narrow range (23–29 kDa) except for PPDTNBT (42 kDa) (Table 1). The polydispersity index (PDI) varies between 1.81 and 2.85. The higher M_n of PPDTNBT suggests a higher reactivity of the corresponding monomers. This might be related to the larger difference between the electron donating and accepting properties of the two monomers, which maximizes for **M3** and **M4**. The similar molecular weights of the polymers allow for a more direct to comparison of their performance in solar cells.

3.2. Optical and Electrochemical Properties

UV-vis absorption spectra of the six PPDTBTs in chloroform solution and as thin film on glass are shown in Figure 1. In thin films, there is a small redshift compared to solution which is attributed to the effects of aggregation of polymer chains. A larger redshift indicates that the degree by which the polymer has aggregated in solution and in film differs more. For PPEDTFBT, we see that the solution spectrum shows more fine structure than the spectrum of the film, although the onsets are virtually identical. We attribute

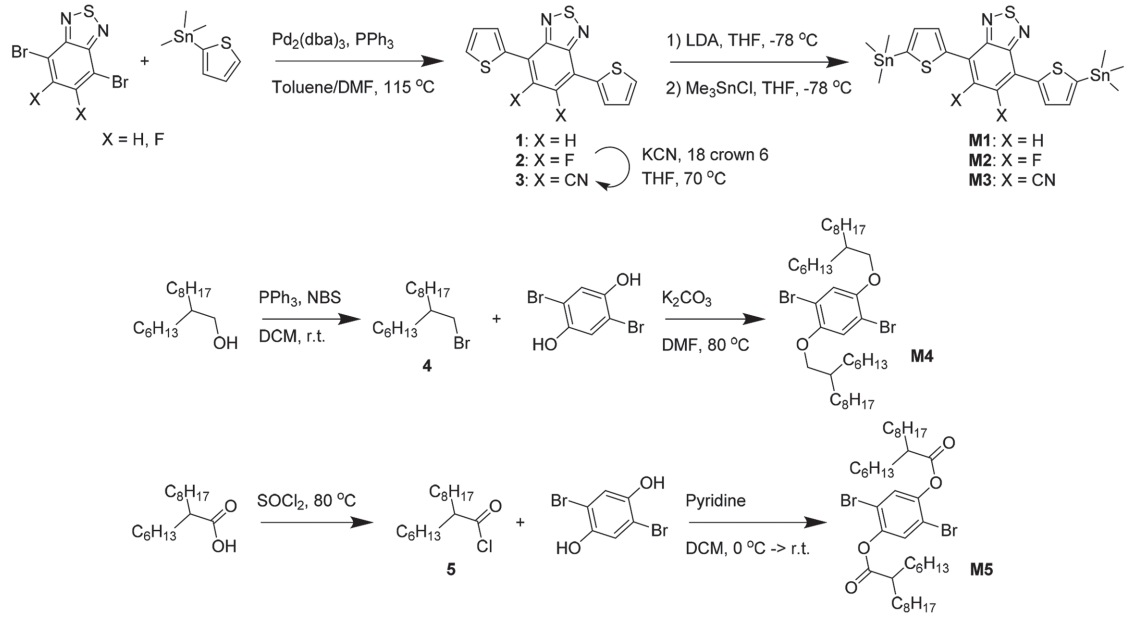

Scheme 1. Synthesis routes toward the H, F, and CN-substituted dithienobenzothiadiazole distannyl monomers (**M1–M3**) and the alkoxy and alkanoate-substituted 1,4-dibromophenylene derivatives (**M4**, **M5**).

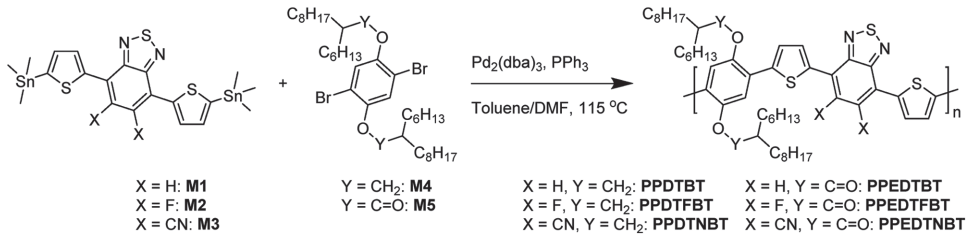

Scheme 2. Polymerization conditions of the six different polymers showing all combinations of monomers **M1–M3** with **M4** and **M5** and the acronyms of the respective polymers.

the peak at 547 nm to dissolved chains and those at 596 and 643 nm to aggregates. This can occur when long chains form well-defined aggregates in solution while the shorter chains are still dissolved. In the film, on the other hand, all chains assemble but in a less ordered fashion, giving rise to broadening of the vibronic structure. The optical band gap in thin films is about 1.75 ± 0.05 eV for all polymers, except for PPDTNBT which has a much smaller band gap (1.47 eV) as a consequence of the stronger charge transfer character of the lowest optical excitation in PPDTNBT compared to the other polymers. PPDTNBT combines the strongest acceptor (**M3**) with the strongest donor (**M4**). This reduces the band gap of these push–pull conjugated polymers.[22, 28–31]

Cyclic voltammetry was performed on thin polymer films deposited on ITO/glass substrates to study the redox levels. The voltammograms (Figure 1b) show in general well-defined redox waves. The onsets of the redox waves are collected in Table 1. The HOMO and LUMO levels decrease with increased electron deficiency of the substituents. Ester substitution on the phenyl moiety or fluorine substitution on benzothiadiazole appears to effect both HOMO and LUMO levels equally (see Figure 1b,c and Figure S1, Supporting Information). On the other hand, nitrile substituents on benzothiadiazole lower the LUMO levels more than the HOMO levels and thereby reduce the electrochemical band gap. A similar observation was made by Heeney and co-workers[26] The differences between optical and electrochemical band gap are about 0.3 eV for most polymers in Table 1. This difference is caused by several effects. First, $E_{g,opt}$ and $E_{g,cv}$ are determined in thin films and in a liquid electrolyte, respectively, that differ strongly in relative permittivity. Second, in the electrochemical experiment electrons are extracted or added but not at the same time, whereas the optical experiment provides the energetic difference for an intramolecular, bound electron–hole state. Finally, there can be morphological differences between the pristine films and those in contact with the liquid electrolyte. These effects are not always equally strong and hence the differences between $E_{g,opt}$ and $E_{g,cv}$ are not constant. For PPEDTFBT, the difference is significantly larger (0.45 eV), while PPEDTNBT shows an almost identical optical and electrochemical band gaps (difference is only 0.06 eV).

3.3. Photovoltaic Devices

Photovoltaic properties of the polymers were studied in regular configuration devices under simulated AM1.5G light (100 mW cm^{-2}). The device stack consisted of an active layer consisting of a bulk heterojunction of the polymer as donor with $PC_{71}BM$ as acceptor, sandwiched between an ITO/PEDOT:PSS hole collecting electrode and

Table 1. Physical, optical, and electronic properties of the PPDTBT polymers.

Polymer	M_n[a)] [kDa]	PDI	$E_{g,opt}$[b)] [eV]	E_{HOMO}[c)] [eV]	E_{LUMO}[c)] [eV]	$E_{g,cv}$ [eV]	Δ_{HOMO}[d)] [eV]	Δ_{LUMO}[d)] [eV]
PPDTBT	23.7	2.85	1.72	–5.20	–3.27	1.93	0.99	0.81
PPDTFBT	28.6	2.09	1.75	–5.34	–3.28	2.06	0.85	0.80
PPDTNBT	42.0	2.09	1.47	–5.64	–3.89	1.75	0.55	0.19
PPEDTBT	27.9	1.81	1.70	–5.37	–3.38	1.99	0.82	0.70
PPEDTFBT	25.6	1.96	1.81	–5.72	–3.46	2.26	0.47	0.62
PPEDTNBT	24.2	2.31	1.76	–5.88	–4.06	1.82	0.31	0.02
$PC_{71}BM$	–		–	–6.19	–4.08	2.11		

[a)]GPC versus polystyrene standards in oDCB at 140 °C; [b)]Low energy absorption onset from pristine polymer thin film spectrum, spin coated from a 6 mg mL^{-1} solution in chloroform at 2000 rpm; [c)]Cyclic voltammetry of thin polymer films on ITO, using 0.1 M $TBA^+PF_6^-$ solution in acetonitrile as electrolyte and versus Fc/Fc^+ as external standard; $E_{HOMO/LUMO} = -q(E_{ox/red} + 5.0)$; [d)]With respect to $PC_{71}BM$.

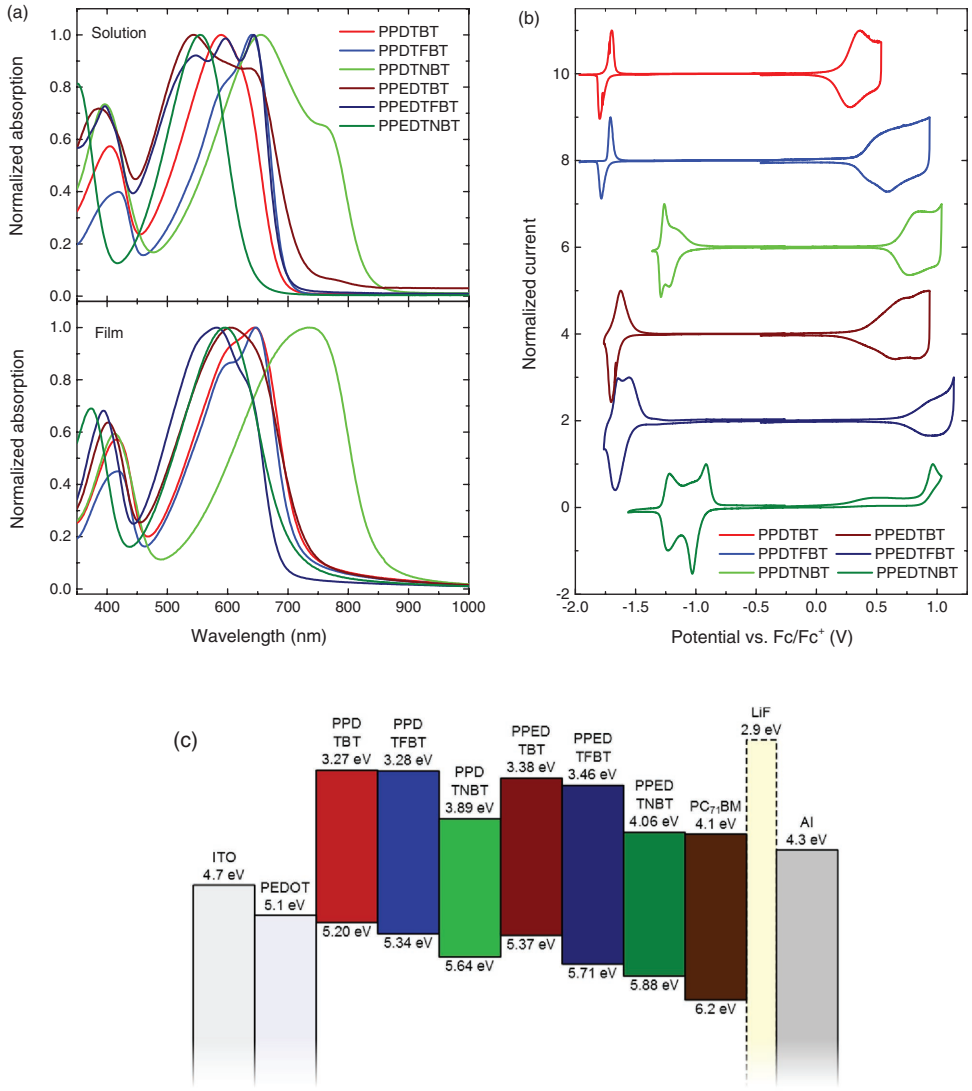

Figure 1. a) Optical absorption spectra of PPDTBT derivatives in chloroform solution (top) and as thin films on glass (bottom). b) Cyclic voltammograms of thin films of PPDTBT derivatives on ITO measured in acetonitrile. c) Electrochemical energy levels for the PPDTBT polymers and work functions of electrode materials in a solar cell.

an LiF-modified aluminum (LiF/Al) electron collecting electrode. Initial devices were made using a 1:1.5 donor/acceptor weight ratio, spin coated from chloroform solution. Device performance was subsequently optimized by using different solvents, cosolvents, and spin coating rates to vary the drying conditions and layer thicknesses. *J*–*V* characteristics and EQEs of the best cells and processing conditions are shown in Figure 2 and Table 2. Device statistics for each material combination can be found in the Table S1 (Supporting Information).

As can be seen in Figure 2 and Table 2, the device performance differs strongly among the different derivatives, especially with respect to the short-circuit photocurrent. We will first discuss the alkoxy-substituted derivatives and then ester-substituted polymers.

For the PPDTBT:$PC_{71}BM$ cells, the highest PCE of 4.9% and the average value of 4.81% ± 0.09% (Table S1, Supporting Information), match rather well with the PCE (best 5.17%, average 5.04%) reported previously by Woo and co-workers,[18] but there is a difference in the fill factor (FF) and V_{oc}. The measured V_{oc} = 0.83 V is higher than expected (0.70 V was found in Ref.[18]) and the FF = 0.53 less (0.63 in Ref.[18]). The EQE spectrum of the PPDTBT:$PC_{71}BM$ cells (Figure 2b) does not show the vibronic structure that can be seen in the absorption spectrum of the pure polymer (Figure 1a). This demonstrates that PPDTBT is less aggregated in the mixed films

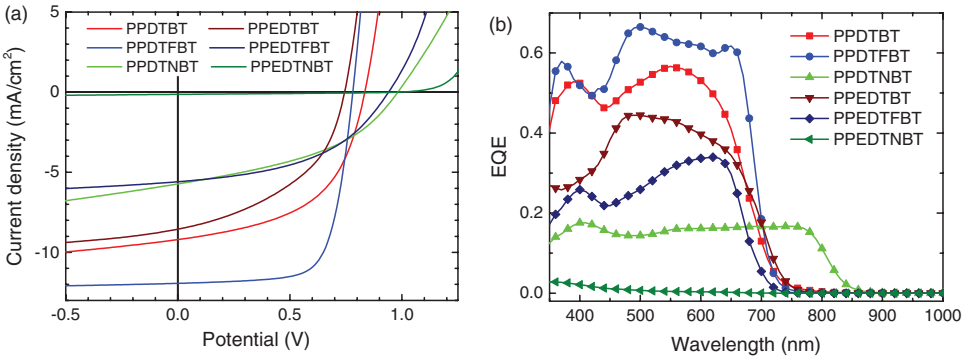

Figure 2. a) *J–V* characteristics of the optimized bulk heterojunction solar cells for the six poly(phenylene-*alt*-dithienobenzothiadiazole)s as donor with $PC_{71}BM$ as acceptor and b) corresponding EQE spectra.

with $PC_{71}BM$ than in pure polymer films. In polymer solar cells the V_{oc} depends on the morphology of the photoactive layer and the extent of aggregation. For a less aggregated polymer, the optical band gap is wider, which results in a deeper HOMO level and, hence, an increased V_{oc}. As we will show below, TEM provides almost featureless images for PPDTBT:$PC_{71}BM$ blends. This indicates intimate mixing of the two components and the absence of phase separated domains. The intimate mixing prevents aggregation and crystallization. In such intimate mixed blends the V_{oc} is higher and the FF is often low (as observed), because bimolecular recombination of charges is enhanced when transport is hampered.

The best performance is found for PPDTFBT:$PC_{71}BM$ cells that reach a PCE of 6.6%, with an average of 6.50% ± 0.12% (Table S1, Supporting Information). This is less than the average efficiency of 8.64% previously by Woo and co-workers[18] for similarly processed PPDTFBT:$PC_{71}BM$ cells. In this case, the difference is exclusively due to a reduced photocurrent. Woo and co-workers[18] found the high performance for 290 nm thick films, while in our case the optimized performance was found for much thinner (87 nm) active layers. The thicker films can absorb more light and hence the photocurrent can be higher. In our hands, the FF and PCE dropped when using thicker PPDTFBT:$PC_{71}BM$ films. The different behavior is possibly related to the lower molecular weight of our sample (M_n = 28.6 kDa) versus the material used by Woo and co-workers[18] (M_n = 42.6 kDa). It is well known that the molecular weight is an important parameter in reaching efficient polymer solar cells.[32–34] Lower molecular weight might in turn be caused by using conventional heating methods during polymerization, rather than microwave heating as was used in the synthesis by Woo and co-workers.[18]

By introducing two nitrile groups instead of two fluorine atoms, the resulting PPDTNBT polymer shows a much deeper (by 0.30 eV) HOMO level and smaller (by 0.28 eV) optical band gap. As a result the V_{oc} of PPDTNBT:$PC_{71}BM$ cells increases to 0.98 V. The combination of such low optical band gap and high V_{oc} results in an E_{loss} of only 0.49 eV (Table 2), which is exceptional for organic solar cells,[20,21,35,36] where E_{loss} commonly exceeds 0.7 eV. When E_{loss} is less than 0.55 eV the EQE usually drops to negligible values, especially for blends with fullerene derivatives.[20] In this sense, the maximum EQE for PPDTNBT:$PC_{71}BM$ cells of still 17% at E_{loss} = 0.49 eV shows that this material is able to generate charges despite a very low driving force.

For the three polymers with a diester-substituted phenylene the HOMO and LUMO levels are further

Table 2. Photovoltaic characteristics of optimized solar cells of PPDTBTs with $PC_{71}BM$.

Polymer	Solvent[a)]	d[b)] [nm]	J_{sc} [mA cm^{-2}]	V_{oc} [V]	FF	PCE [%]	E_{loss} [eV]
PPDTBT	oDCB	71	11.2	0.83	0.53	4.9	0.89
PPDTFBT	2% DPE in CB	87	12.0	0.78	0.71	6.6	0.97
PPDTNBT	2% DIO in CF	68	4.3	0.98	0.42	1.8	0.49
PPEDTBT	20% oDCB in CF	99	7.8	0.74	0.46	2.7	0.96
PPEDTFBT	2% DPE in CB	94	5.4	0.94	0.47	2.4	0.87
PPEDTNBT	2% DIO in CF		0.1[c)]	0.98	0.33	0.04[c)]	0.78

[a)]Solvents used are chloroform (CF), chlorobenzene (CB), oDCB, diphenyl ether (DPE), and 1,8-diiodooctane (DIO); [b)]Active layer thickness; [c)]J_{sc} and PCE not corrected for spectral response.

lowered compared to the corresponding alkoxy derivatives (Figure 1 and Table 2). Hence the fact that for the optimized PPEDTBT:$PC_{71}BM$ cells, the V_{oc} = 0.74 V is less than that of PPDTBT:$PC_{71}BM$ cells, with V_{oc} = 0.83 V is unexpected. For PPEDTBT:$PC_{71}BM$ cells the V_{oc} is correlated with the extent of aggregation of the polymers in the photoactive layers. When processed from chloroform with 20% oDCB as cosolvent, the V_{oc} is 0.74 V, but this increases substantially to V_{oc} = 0.99 V when 2% 1,8-diiodooctane (DIO) was used as cosolvent (Figure S2a, Supporting Information). The onset of the EQE spectra shifts by 40 nm toward lower wavelengths (Figure S2b, Supporting Information), demonstrating reduced aggregation of PPEDTBT when cast using DIO as cosolvent. The larger optical band gap increases V_{oc}. The increase in V_{oc}, is, however, accompanied by a loss in J_{sc} from 7.8 to 3.0 mA cm^{-2}, such that the PCE of the cell made with 2% DIO as cosolvent is lower.

For PPEDTFBT:$PC_{71}BM$ cells the V_{oc} has increased compared to the corresponding alkoxy-substituted analogue (PPDTFBT:$PC_{71}BM$), but J_{sc}, FF, and PCE are less (Table 2). When comparing the two materials PPEDTFBT and PPDTFBT, we see that replacing the alkoxy side chains by ester side chains has resulted in a small increase (≈0.06 eV) in the optical band gap and a significant increase (0.16 V) in V_{oc}, such that the energetic loss term E_{loss} decreases from 0.97 to 0.87 eV. This energetic improvement is, however, counteracted by the reduction in photocurrent and loss in EQE by a factor of two.

The nitrile/ester-substituted PPEDTNBT polymer has HOMO and LUMO levels that are too close to those of $PC_{71}BM$ to expect any electron transfer and the photocurrent is negligible.

3.4. Morphology

The morphology of the active layers was studied using TEM. TEM images of the active layers of the optimized solar cells are shown in Figure 3. TEM images of active layers from pure chloroform are shown in Figure S3 (Supporting Information). All solar cells benefitted significantly from the addition of a cosolvent or using a solvent different from chloroform (Table S1, Supporting Information). When cast from pure chloroform most photoactive layers exhibit large (≈100 nm) dark $PC_{71}BM$-rich domains in TEM that are formed as a consequence of liquid–liquid demixing during drying.[37,38] As a consequence the performance remains low (Table S1, Supporting Information). In the optimized solar cells the length scale of phase separation is much smaller. As noted above, the PPDTBT:$PC_{71}BM$ layer is a finely dispersed blend of the two components with no signs of crystallinity. In contrast, the optimized PPDTFBT:$PC_{71}BM$ blend clearly shows a crystalline fibrillar network that is known to produce well performing photovoltaic devices by providing domains that are both small enough for efficient charge separation as well as pure enough to prevent recombination.[34] The TEM image at higher magnification shows regions in which lattice fringes are apparent (inset

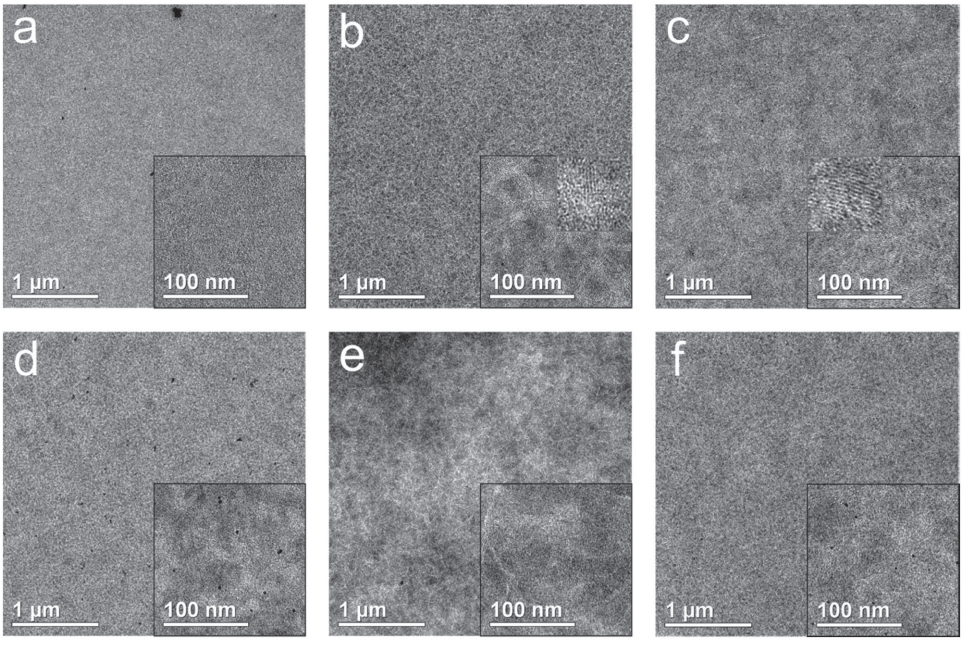

Figure 3. Bright-field TEM morphology images of solar cells consisting of optimized active layers. a) PPDTBT:$PC_{71}BM$, b) PPDTFBT:$PC_{71}BM$, c) PPDTNBT:$PC_{71}BM$, d) PPEDTBT:$PC_{71}BM$, e) PPEDTFBT:$PC_{71}BM$, and f) PPEDTNBT:$PC_{71}BM$.

of Figure 3b) that evidence the semicrystalline nature of the polymer. The other layers also show a certain degree of crystallinity, with the exception of the PPEDTNBT:$PC_{71}BM$ blend, but the extensive network formation as is seen for the PPDTFBT:$PC_{71}BM$ blend, is not observed. In intimately mixed blends in which the polymer domains are small and less crystalline, charge transport is hindered by the absence of efficient charge percolation pathways, such that bimolecular recombination of charges limits the J_{sc} and FF. The tendency of a polymer to crystallize in these blends with $PC_{71}BM$ is governed by the molecular structure, the molecular weight of the polymer, and the solubility of the polymer in the solvents used for casting the films.[34]

3.5. Effect of Photon Energy Loss

It is of interest to relate the performance of the solar cells to the energy level offsets between the HOMO levels (Δ_{HOMO}) and LUMO levels (Δ_{LUMO}) of the donor polymers and the fullerene acceptor. Empirical studies have shown that Δ_{HOMO} and Δ_{LUMO} should both be about 0.3 eV to facilitate photoinduced charge transfer from the polymer donor to the fullerene acceptor or vice versa.[39] In fact, Δ_{HOMO} and Δ_{LUMO} represent energy losses and hence reducing Δ_{HOMO} and Δ_{LUMO} while keeping a high efficiency for photoinduced electron transfer is a way to reduce energy losses in organic solar cells and enhance PCEs. As can be seen in Table 1, all polymers in this study, except the two nitrile-substituted derivatives, fulfill the criterion that $\Delta_{HOMO} >$ 0.3 eV *and* $\Delta_{LUMO} > 0.3$ eV. Introducing stronger electron withdrawing substituents on the benzothiadiazole (i.e., going from H, F, to CN) results in a reduction of both Δ_{HOMO} and Δ_{LUMO}. In fact, the effect of nitrile substitution appears to be too large, resulting in a Δ_{LUMO} that becomes too small for efficient photoinduced electron transfer to occur. Hence, the contribution of the polymer to the EQE of PPDTNBT:$PC_{71}BM$ cells ($\Delta_{LUMO} = 0.19$ eV) is reduced to 17% and becomes virtually 0% for PPEDTNBT:$PC_{71}BM$ cells ($\Delta_{LUMO} = 0.02$ eV). The Δ_{HOMO} governs photoinduced electron transfer from the donor HOMO to the HOMO of the excited acceptor. This process is also commonly referred to as hole transfer. For polymer–fullerene solar cells, this hole transfer can be quantified from the EQE in the region where the fullerene absorbs light (400–650 nm). As can be seen in Table 1 and Figure 2b, the EQE at about 480 nm remains high when $\Delta_{HOMO} > 0.6$ eV but is already reduced when Δ_{HOMO} drops below 0.6 eV. At $\Delta_{HOMO} = 0.3$ eV the contribution of the fullerene to the photocurrent vanishes in PPEDTNBT:$PC_{71}BM$ cells.

While, Δ_{LUMO} and Δ_{HOMO} are useful parameters to understand the contributions of light absorbed by the donor or the acceptor to the photocurrent, their use is somewhat hampered by the fact that it remains a challenge to determine the HOMO and LUMO levels accurately. Even if that would be the case, it remains debatable to which extent these values can be used when the optical band gap $E_{g,opt}$ and the HOMO–LUMO gap differ considerably (Note that Table 1 shows that $E_{g,cv} > E_{g,opt}$ and that the difference is not constant). A more reliable way to relate the EQE to the energetic losses is therefore comparing the optical band gap to the open-circuit voltage. The resulting photon energy loss parameter, E_{loss}, represents the minimum energy loss that a photon incurs when converted into a photovoltage. The challenge for a high PCE is to achieve a low E_{loss} in combination with a high EQE.

The aim of this study was to see if the relatively high E_{loss} of the PPDTBT and PPDTFBT polymers described by Woo and co-workers[18] could be reduced, by using nitrile groups on the benzothiadiazole or by ester groups on the phenylene ring. Table 2 shows that the ester groups on the phenylene ring indeed reduce E_{loss} for PPDTFBT but not for PPDTBT, because for PPDTBT and its ester-substituted analogue PPEDTBT the V_{oc} strongly depends on the extent of aggregation. Introduction of the two nitrile groups on benzothiadiazole lowers E_{loss} for PPDTNBT (0.49 eV) as compared to PPDTBT (0.89 eV) and PPDTFBT (0.97 eV), but the PCE did not improve because the photocurrent and fill factor decreased. At lower E_{loss} the driving force for electron transfer is reduced, which reduces the quantum efficiency for charge generation and, hence, reduces J_{sc}. Especially for $E_{loss} < 0.6$ eV, J_{sc} is known to drop quickly.[19] The higher E_{loss} for PPDTBT and PPDTFBT ensures more efficient charge generation after photoexcitation and the effect of the much increased J_{sc} outweighs the lower V_{oc}. Despite a relatively low PCE of 1.8%, PPDTNBT:$PC_{71}BM$ emerges as an interesting material combination from an energetic point of view. The E_{loss} of this material is effectively lowered to 0.49 eV by substituting the benzothiadiazole with nitrile groups and thereby lowering the HOMO and LUMO levels. This E_{loss} represents one of the lowest values reported to date for a working organic solar cell. The EQE of ≈17% is quite small[20,21] but demonstrates that charges can still be generated under minimal driving force. Further improvement of the EQE and PCE may be achieved when a more phase-separated morphology could be realized. To achieve this, solubilizing side chains, molecular weight, and polydispersity are parameters to vary next to exploring different processing conditions.

4. Conclusions

In summary, six poly(phenylene-*alt*-dithienobenzothiadiazole)-based polymers have been synthesized using different electron withdrawing substituents on the donor and acceptor moieties. The use of hydrogen, fluorine, or nitrile substitution on the benzothiadiazole and the use

of alkoxy or ester substitution on the phenylene moiety provide an effective way of lowering and tuning the HOMO and LUMO energy levels. Introduction of a more electronegative substituent lowered both HOMO and LUMO levels almost equally, except for nitrile substitution that affected the LUMO level more strongly. With the lowered HOMO energy levels, the open-circuit voltage of photovoltaic cells made with the poly(phenylene-*alt*-dithienobenzothiadiazole)-based polymers as donor and $PC_{71}BM$ as acceptor can be increased. As a result, the photon energy loss that is incurred in these devices can be reduced. In the best device, based on PPDTFBT:$PC_{71}BM$, the PCE reaches 6.6%. Although the other polymers provide a reduced photon energy loss (E_{loss}) in solar cells and therefore present more favorable energetics, their PCEs are actually not increased because of lower external quantum efficiencies and fill factors that are related to their less phase-separated morphology and reduced aggregation into semicrystalline domains. The PPDTNBT:$PC_{71}BM$ solar cells represent an interesting case. This material has one of the lowest E_{loss} = 0.49 eV reported to date, while still having a substantial EQE of 17%. Further optimization of this material, e.g., by varying the solubilizing side chains, might provide improved morphologies and higher PCEs.

Supporting Information

Supporting Information is available from the Wiley Online Library or from the author.

Acknowledgements: The research had received funding from the European Research Council under the European Union's Seventh Framework Programme (FP/2007-2013)/European Research Council Grant Agreement No. 339031 and from the Ministry of Education, Culture and Science (Gravity program 024.001.035). This research forms part of the research programme of the Dutch Polymer Institute (DPI), project #734.

Received: October 21, 2016; Revised: December 11, 2016; Published online: January 24, 2017; DOI: 10.1002/macp.201600502

Keywords: energy loss; fullerenes; morphology; organic solar cells; semiconducting polymer

[1] Z. He, B. Xiao, F. Liu, H. Wu, Y. Yang, S. Xiao, C. Wang, T. P. Russell, Y. Cao, *Nat. Photonics* **2015**, *9*, 174.
[2] X. Ouyang, R. Peng, L. Ai, X. Zhang, Z. Ge, *Nat. Photonics* **2015**, *9*, 520.
[3] Y. Liu, J. Zhao, Z. Li, C. Mu, W. Ma, H. Hu, K. Jiang, H. Lin, H. Ade, H. Yan, *Nat. Commun.* **2014**, *5*, 529.
[4] R. S. Ashraf, I. Meager, M. Nikolka, M. Kirkus, M. Planells, B. C. Schroeder, S. Holliday, M. Hurhangee, C. B. Nielsen, H. Sirringhaus, I. McCulloch, *J. Am. Chem. Soc.* **2015**, *137*, 1314.
[5] D. Mühlbacher, M. Scharber, M. Morana, Z. Zhu, D. Waller, R. Gaudiana, C. Brabec, *Adv. Mater.* **2006**, *18*, 2884.
[6] K. H. Hendriks, W. Li, M. M. Wienk, R. A. J. Janssen, *J. Am. Chem. Soc.* **2014**, *136*, 12130.
[7] W. Li, K. H. Hendriks, W. S. C. Roelofs, Y. Kim, M. M. Wienk, R. A. J. Janssen, *Adv. Mater.* **2013**, *25*, 3182.
[8] E. Zhou, Q. Wei, S. Yamakawa, Y. Zhang, K. Tajima, C. Yang, K. Hashimoto, *Macromolecules* **2010**, *43*, 821.
[9] L. Dou, C.-C. Chen, K. Yoshimura, K. Ohya, W.-H. Chang, J. Gao, Y. Liu, E. Richard, Y. Yang, *Macromolecules* **2013**, *46*, 3384.
[10] W. Li, A. Furlan, K. H. Hendriks, M. M. Wienk, R. A. J. Janssen, *J. Am. Chem. Soc.* **2013**, *135*, 5529.
[11] J. Zhao, Y. Li, G. Yang, K. Jiang, H. Lin, H. Ade, W. Ma, H. Yan, *Nat. Energy* **2016**, *1*, 15027.
[12] H. Hu, K. Jiang, G. Yang, J. Liu, Z. Li, H. Lin, Y. Liu, J. Zhao, J. Zhang, F. Huang, Y. Qu, W. Ma, H. Yan, *J. Am. Chem. Soc.* **2015**, *137*, 14149.
[13] J. You, L. Dou, K. Yoshimura, T. Kato, K. Ohya, T. Moriarty, K. Emery, C.-C. Chen, J. Gao, G. Li, Y. Yang, *Nat. Commun.* **2013**, *4*, 1446.
[14] C. C. Chen, W. H. Chang, K. Yoshimura, K. Ohya, J. You, J. Gao, Z. Hong, Y. Yang, *Adv. Mater.* **2014**, *26*, 5670.
[15] J. Y. Kim, K. Lee, N. E. Coates, D. Moses, T.-Q Nguyen, M. Dante, A. J. Heeger, *Science* **2007**, *317*, 222.
[16] H. Zhou, L. Yang, A. C. Stuart, S. C. Price, S. Liu, W. You, *Angew. Chem., Int. Ed.* **2011**, *50*, 2995.
[17] A. C. Stuart, J. R. Tumbleston, H. Zhou, W. Li, S. Liu, H. Ade, W. You, *J. Am. Chem. Soc.* **2013**, *135*, 1806.
[18] T. L. Nguyen, H. Choi, S.-J. Ko, M. A. Uddin, B. Walker, S. Yum, J.-E. Jeong, M. H. Yun, T. J. Shin, S. Hwang, J. Y. Kim, H. Y. Woo, *Energy Environ. Sci.* **2014**, *7*, 3040.
[19] W. Li, W. S. C. Roelofs, M. M. Wienk, R. A. J. Janssen, *J. Am. Chem. Soc.* **2012**, *134*, 13787.
[20] W. Li, K. H. Hendriks, A. Furlan, M. M. Wienk, R. A. J. Janssen, *J. Am. Chem. Soc.* **2015**, *137*, 2231.
[21] K. Kawashima, Y. Tamai, H. Ohkita, I. Osaka, K. Takimiya, *Nat. Commun.* **2015**, *6*, 10085.
[22] T. H. Lee, M. A. Uddin, C. Zhong, S.-J. Ko, B. Walker, T. Kim, Y. J. Yoon, S. Y. Park, A. J. Heeger, H. Y. Woo, J. Y. Kim, *Adv. Energy Mater.* **2016**, *6*, 1600637.
[23] J.-F. Jheng, Y.-Y. Lai, J.-S. Wu, Y.-H. Chao, C.-L. Wang, C.-S. Hsu, *Adv. Mater.* **2013**, *25*, 2445.
[24] L. Biniek, C. L. Chochos, N. Leclerc, O. Boyron, S. Fall, P. Lévèque, T. Heiser, *J. Polym. Sci., Part A: Polym. Chem.* **2012**, *50*, 1861.
[25] J. E. Carlé, J. W. Andreasen, M. Jørgensen, F. C. Krebs, *Sol. Energy Mater. Sol. Cells* **2010**, *94*, 774.
[26] A. Casey, Y. Han, Z. Fei, A. J. P. White, T. D. Anthopoulos, M. Heeney, *J. Mater. Chem. C* **2015**, *3*, 265.
[27] A. Casey, S. D. Dimitrov, P. Shakya-Tuladhar, Z. Fei, M. Nguyen, Y. Han, T. D. Anthopoulos, J. R. Durrant, M. Heeney, *Chem. Mater.* **2016**, *28*, 5110.
[28] H. Zhou, L. Yang, W. You, *Macromolecules* **2012**, *45*, 607.
[29] C. Kitamura, S. Tanaka, Y. Yamashita, *Chem. Mater.* **1996**, *8*, 570.
[30] E. E. Havinga, W. ten Hoeve, H. Wynberg, *Polym. Bull.* **1992**, *29*, 119.
[31] E. E. Havinga, W. ten Hoeve, H. Wynberg, *Synth. Met.* **1993**, *55–57*, 299.

[32] R. C. Coffin, J. Peet, J. Rogers, G. C. Bazan, *Nat. Chem.* **2009**, *1*, 657.
[33] S. Wakim, S. Beaupré, N. Blouin, B.-R. Aich, S. Rodman, R. Gaudiana, Y. Tao, M. Leclerc, *J. Mater. Chem.* **2009**, *19*, 5351.
[34] J. J. van Franeker, G. H. L. Heintges, C. Schaefer, G. Portale, W. Li, M. M. Wienk, P. van der Schoot, R. A. J. Janssen, *J. Am. Chem. Soc.* **2015**, *137*, 11783.
[35] K. Gao, L. Li, T. Lai, L. Xiao, Y. Huang, F. Huang, J. Peng, Y. Cao, F. Liu, T. Russell, R. Janssen, X. Peng, *J. Am. Chem. Soc.* **2015**, *137*, 7282.
[36] M. Wang, H. Wang, T. Yokoyama, X. Liu, Y. Huang, Y. Zhang, T.-Q. Nguyen, S. Aramaki, G. C. Bazan, *J. Am. Chem. Soc.* **2014**, *136*, 12576.
[37] S. Kouijzer, J. J. Michels, M. van den Berg, V. S. Gevaerts, M. Turbiez, M. M. Wienk, R. A. J. Janssen, *J. Am. Chem. Soc.* **2013**, *135*, 12057.
[38] J. J. van Franeker, M. Turbiez, W. Li, M. M. Wienk, R. A. J. Janssen, *Nat. Commun.* **2015**, *6*, 6229.
[39] M. C. Scharber, D. Mühlbacher, M. Koppe, P. Denk, C. Waldauf, A. J. Heeger, C. J. Brabec, *Adv. Mater.* **2006**, *18*, 789.